

## Soliton dynamics in a 2D lattice model with nonlinear interactions

This article has been downloaded from IOPscience. Please scroll down to see the full text article.

2003 J. Phys. A: Math. Gen. 36 643

(<http://iopscience.iop.org/0305-4470/36/3/304>)

View [the table of contents for this issue](#), or go to the [journal homepage](#) for more

Download details:

IP Address: 171.66.16.86

The article was downloaded on 02/06/2010 at 16:24

Please note that [terms and conditions apply](#).

# Soliton dynamics in a 2D lattice model with nonlinear interactions

T Ioannidou<sup>1,3</sup>, J Pouget<sup>1</sup> and E Aifantis<sup>2,4</sup>

<sup>1</sup> Laboratoire de Modélisation en Mécanique (associé au CNRS), Université Pierre et Marie Curie, Tour 66, 4 place Jussieu, 75252 Paris Cédex 05, France

<sup>2</sup> Laboratory of Mechanics and Materials, Polytechnic School, Aristotle University of Thessaloniki, 54006, Thessaloniki, Greece

Received 16 October 2002, in final form 20 November 2002

Published 7 January 2003

Online at [stacks.iop.org/JPhysA/36/643](http://stacks.iop.org/JPhysA/36/643)

## Abstract

This paper is concerned with a lattice model which is suited to square–rectangle transformations characterized by two strain components. The microscopic model involves nonlinear and competing interactions, which play a key role in the stability of soliton solutions and emerge from interactions as a function of particle pairs and noncentral type or bending forces. Special attention is devoted to the continuum approximation of the two-dimensional discrete system with the view of including the leading discreteness effects at the continuum description. The long-time evolution of the localized structures is governed by an asymptotic integrable equation of the Kadomtsev–Petviashvili I type which allows the explicit construction of moving multi-solitons on the lattice. Numerical simulation performed at the discrete system investigates the stability and dynamics of the multi-soliton in the lattice space.

PACS numbers: 05.50.+q, 05.45.Yn

## 1. Introduction

Considerable interest has recently been devoted to spatio-temporal patterns as well as the associated defects and dynamics such as standing-wave patterns, localized structures including solitons or oscillating patterns. These structures become fundamental in the study of phase transitions which are usually accompanied by the appearance of defects: dislocation motions, grain boundaries, domain wall structures and twinings [1–3]. One of the aims of the present research is to understand how solitons arising at the microscale (i.e. at the level of the lattice model) are able to organize the system at the macroscale and what the selection properties of

<sup>3</sup> Permanent address: Institute of Mathematics, University of Kent, Canterbury CT2 7NF, UK.

<sup>4</sup> Center for Mechanics of Materials and Instabilities, Michigan Technological University, Houghton, MI 49931, USA.

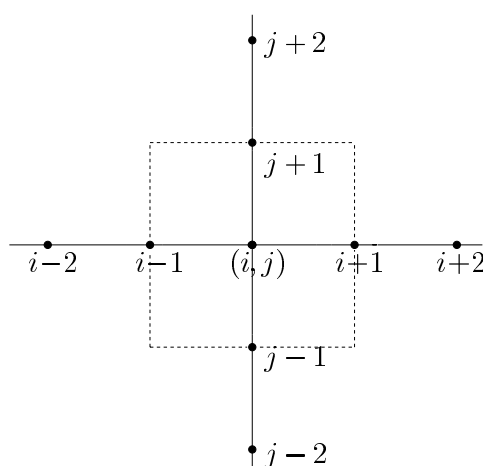


**Figure 1.** Two-dimensional lattice model with the detail of interatomic interactions between the first and second neighbours in the  $i, j$  directions.

the nonlinear structures are. The present work is particularly motivated by the existence of solitonic structures occurring in phase transformations in crystalline alloys.

The same lattice model has been successfully used to examine the formation of localized strain patterns decaying in all directions [4–6]. Then the corresponding research results in the partial softening of the transverse-acoustic phonon branch at a nonzero wave number; the positive curvature of the dispersion branch at the long wavelength limit; and the shearing motion of the atomic planes along the stacking direction leading to spatially arranged structures made of martensitic twin bands and the existence of strain solitary waves describing the coherent movement of martensitic domains. More precisely, the nonlinear dynamics of the two-dimensional model allows us to examine the stability of the lattice using numerical simulations which have shown the formation of localized strain structures emerging from an instability mechanism [4, 6].

In the present paper we continue the investigation of the properties of the two-dimensional lattice model in order to study the existence, stability and dynamics of lattice multi-soliton configurations. In fact, the study provides the critical values of the coefficients of the lattice model for which lattice solitons exist and move along the plane, using the fact that the continuum limit of the long-time evolution of the patterns is governed by an asymptotic equation of the Kadomtsev–Petviashvili I type. Recently in [7], the Kadomtsev–Petviashvili equation has been derived for quasilattice waves by considering oscillations of a two-dimensional square lattice array of atoms with interactions only between the nearest neighbours.

This paper is organized as follows: in section 2 we introduce the lattice model, while in section 3 we deal with its continuum approximation and show that it leads to the Kadomtsev–Petviashvili I equation for long-time evolution. Finally, in section 4 numerical simulations of the discrete model based on the Kadomtsev–Petviashvili I multi-solitons are performed and their dynamics are discussed in some detail.

## 2. Lattice model

Let us consider an atomic plane made of squares parallel to the  $i$  and  $j$  directions presented in figure 1. Such a lattice model can be extracted from the cubic lattice of crystalline alloys

(such as the fcc symmetry of In–Tl, Fe–Pd and other crystals). The model describes a cubic tetragonal transformation of the lattice. A particle of the lattice plane is located by  $(i, j)$ . After deformation of the lattice, the particle undergoes a displacement defined by  $u_{i,j} = u(i, j)$  along the  $i$  and  $j$  directions.

The particles interact via two kinds of interatomic potentials: (i) interactions between first nearest neighbours considered as functions of the particle pairs in the  $i$  and  $j$  diagonal directions and (ii) interactions involving noncentral forces or three-body interactions between the first nearest and second nearest neighbours in the  $i$  and  $j$  directions. The potential describing the first interactions possesses stable, unstable or metastable states according to a control parameter which is connected with temperature [8]. The latter interactions amount to describing, at the microscopic level, the resistance of the crystalline cell to twisting and bending [4, 5] and thus provide competing interactions [9, 10]. The noncentral interactions are of particular interest for the competing interactions and stability of the nonlinear structures. On using the invariance of the lattice energy under translations and rotations, the following potential functional was introduced in [6],

$$\mathcal{V} = \sum_{(i,j)} \left[ \Phi S_{i,j} + \frac{\beta}{2} G_{i,j}^2 + \frac{\delta}{2} \{ (\Delta_L^+ S_{i,j})^2 + (\Delta_T^+ G_{i,j})^2 \} + \frac{\eta}{2} \{ (\Delta_L^+ [S_{i+1,j} + 2S_{i,j} + S_{i-1,j}])^2 + \{ \Delta_T^+ [G_{i+1,j} + 2G_{i,j} + G_{i-1,j}] \}^2 \} \right] \quad (2.1)$$

where the discrete deformations are defined as

$$S_{i,j} = u_{i,j} - u_{i-1,j} \quad G_{i,j} = u_{i,j} - u_{i,j-1} \quad (2.2)$$

and the potential  $\Phi$  is given by

$$\Phi(S_{i,j}) = \frac{1}{2} \alpha_1 S_{i,j}^2 - \frac{1}{3} \alpha_2 S_{i,j}^3. \quad (2.3)$$

For simplicity, the lattice energy (2.1) has been chosen to be dimensionless. The first and second terms in (2.1) represent the nonlinear and linear potentials coming from the particle pair interactions where  $(\alpha_1, \alpha_2)$  and  $\beta$  are the lattice force coefficients for the longitudinal and shear deformations, respectively. The third and fourth parts of (2.1) hold for the actions of the noncentral interactions in the  $i$  and  $j$  directions. The interactions are characterized by the parameters  $\delta$  and  $\eta$  for the actions between first and second nearest particles, respectively. On the other hand, the operators  $\Delta_L^+$  and  $\Delta_T^+$  hold for the forward first-order finite difference in the  $i$  and  $j$  directions:  $\Delta_L^+ S_{i,j} = S_{i+1,j} - S_{i,j}$  and  $\Delta_T^+ G_{i,j} = G_{i,j+1} - G_{i,j}$ .

**Remark.** Due to (2.2) the noncentral interactions in (2.1) are of the form  $u_{i-1,j} + u_{i+1,j} - 2u_{i,j}$  for the first nearest neighbour interaction and of the form  $u_{i-2,j} + u_{i+2,j} - 2u_{i,j}$  for the second nearest neighbour interaction (the same for the  $G_{i,j}$  deformation).

In addition, a one-dimensional version of the model can be obtained, reduced from the complete two-dimensional one, in which the shearing motion of the atomic planes along the stacking direction is modelled by arrays of martensitic and austenitic solitary waves. This reduced system has been examined in detail, and it has been observed that localized structures emerge as arrays of elastic solitary waves [4, 5].

By introducing the kinetic energy associated with the displacement  $u_{i,j}$  (for unit mass) as

$$\mathcal{T} = \sum_{(i,j)} \frac{1}{2} \dot{u}_{i,j}^2 \quad (2.4)$$

the corresponding difference-differential equations of motion for  $u_{i,j}$ , deduced from the Hamiltonian  $H = \mathcal{T} + \mathcal{V}$ , are given by

$$\ddot{u}_{i,j} = \Delta_L^+ \Sigma_{L_{i,j}} + \Delta_T^+ \Sigma_{T_{i,j}} \quad (2.5)$$

where the discrete stresses are defined as

$$\Sigma_{L_{i,j}} = \sigma_{i,j} - \Delta_L^- \chi_{L_{i,j}} \quad (2.6)$$

$$\Sigma_{T_{i,j}} = \beta G_{i,j} - \Delta_T^- \chi_{T_{i,j}} \quad (2.7)$$

$$\sigma_{i,j} = \alpha_1 S_{i,j} - \alpha_2 S_{i,j}^2 \quad (2.8)$$

$$\chi_{L_{i,j}} = \Delta_L^+ \{\delta S_{i,j} + \eta[S_{i+2,j} + 4S_{i+1,j} + 6S_{i,j} + 4S_{i-1,j} + S_{i-2,j}]\} \quad (2.9)$$

$$\chi_{T_{i,j}} = \Delta_T^+ \{\delta G_{i,j} + \eta[G_{i,j+2} + 4G_{i,j+1} + 6G_{i,j} + 4G_{i,j-1} + G_{i,j-2}]\}. \quad (2.10)$$

Equations (2.6) and (2.7) correspond to the discrete macroscopic stresses due to the fact that the deformations  $S_{i,j}$  and  $G_{i,j}$  are functions of the discrete displacements  $u_{i,j}$ . Note that the stress (2.8) which follows from the potential  $\Phi$  since  $\sigma_{i,j} = \partial\Phi/\partial S_{i,j}$  is nonlinear in terms of the strain  $S_{i,j}$ . Also, the microscopic stresses (2.9) and (2.10) emerging from the noncentral forces are functions of the discrete variations of the deformations  $S_{i,j}$  and  $G_{i,j}$  in the  $i$  and  $j$  directions, respectively.

Due to the strong nonlinear nature of the problem, these equations are not manageable except for the linear problem which has been examined in [11]. In this paper, these equations are solved using numerical simulations with appropriate initial and boundary conditions. More precisely, using the continuum approximation a quasi-continuum model has been obtained which includes the leading discreteness effects and allows us to investigate the existence of soliton configurations and study their dynamics.

### 3. Continuum approximation

In order to describe the lattice dynamics at the quasi-continuum scale we assume that the discrete functions are slowly varying over the lattice spacing. In fact, both the deformations (2.2) have been expanded using Taylor's series up to third order, that is  $S = hu_x - \frac{h^2}{2}u_{xx} + \frac{h^3}{6}u_{xxx}$  (where  $h$  is the lattice spacing); while all other terms have been expanded for long wavelength up to fourth order. After some classical algebras the continuum equations of motion for the deformation  $u(x, y, t)$  are

$$u_{tt} = \alpha_1 u_{xx} - \alpha_2 (u^2)_{xx} + \delta_L u_{xxxx} + \delta_T u_{yyyy} + \beta u_{yy} \quad (3.11)$$

for dimensionless space units, i.e. rescaling  $x \rightarrow x/h$  and  $y \rightarrow y/h$ . The coefficients  $\delta_L$  and  $\delta_T$  are given in terms of the coefficients of the model, i.e.

$$\delta_L = \frac{\alpha_1}{12} - \delta - 16\eta \quad \delta_T = \frac{\beta}{12} - \delta - 16\eta. \quad (3.12)$$

#### 3.1. Asymptotic model

In order to understand the evolution of the localized structures over a large time scale of the order of  $\varepsilon^{-1}$  and for a weakly nonlinear medium, we consider the asymptotic equation derived from the continuum equation (3.11). By assuming that the contribution of the nonlinear term is weak throughout we rescale the nonlinear and dispersive terms by introducing a small parameter  $\varepsilon < 1$  as follows:

$$\alpha_2 = \varepsilon \bar{\alpha} \quad \delta_L = \varepsilon \bar{\delta}_L \quad \delta_T = \varepsilon \bar{\delta}_T. \quad (3.13)$$

Then for large times (of order  $\varepsilon^{-1}$ ), the asymptotic expansion of the displacement field is

$$u(x, y, t) = u_0(\xi, Y, \tau) + \varepsilon u_1(x, y, t) + O(\varepsilon^2) \quad (3.14)$$

where  $\xi = x - ct$  is the stretch phase variable,  $Y = \varepsilon^{1/2}y$  is the stretch transverse variable and  $\tau = \varepsilon t$  is the slow time variable.

Using equations (3.13) and (3.14) and keeping terms of order  $\varepsilon$  only, equation (3.11) becomes

$$2cu_{0\xi} - \bar{\alpha} \left( u_0^2 \right)_\xi + \bar{\delta}_L u_{0\xi\xi\xi} + \beta u_{0YY} = u_{l_t} - \alpha_1 u_{1xx} - \beta u_{1yy} \quad (3.15)$$

where we have set the sound velocity in the  $x$  direction to be equal to  $c = \sqrt{\alpha_1}$  (for  $\alpha_1 > 0$ ).

Then the secularity condition [12] implies that both the left- and right-hand sides of (3.15) are to equal zero. Thus, the right-hand side leads to the standard two-dimensional linear wave equation for  $u_1$ , while the left-hand side gives the long-time evolution of  $u_0$  defined by

$$\left( u_{0\tau} + \bar{\alpha} \left( u_0^2 \right)_\xi + \bar{\delta}_L u_{0\xi\xi\xi} \right)_\xi = \beta u_{0YY}. \quad (3.16)$$

Note that the following change of variables and parameters have been considered:  $T = -\tau/2c$  and  $\bar{\delta}_L = -\delta_L$  in order that (3.16) transforms into a standard form, and that for specific choices of the parameters  $\bar{\alpha}$ ,  $\bar{\delta}_L$  and  $\beta > 0$  equation (3.16) becomes the Kadomtsev–Petviashvili I equation [13] (see later). Note that equation (3.16) was first derived in [6] using Fourier images.

### 3.2. The Kadomtsev–Petviashvili equations

Nonlinear quasi-one-dimensional waves (with  $y$  much larger than  $x$ ) in a weakly dispersive medium are described by the dimensionless Kadomtsev–Petviashvili (KP) equations

$$(u_t + 3(u^2)_x + u_{xxx})_x = \pm u_{yy} \quad (3.17)$$

where the  $\pm$  on the right-hand side is determined by the dispersive property of the system; i.e. the upper sign is usually referred to as positive dispersion and the corresponding equation is known as KPI (which is the case we study here).

The exact multi-soliton solutions of KPI can be constructed by different methods (see, for example, [14, 15]). For our purposes it is convenient to write them in the Hirota form, i.e.

$$u(x, y, t) = 2 \frac{\partial^2}{\partial x^2} \ln \phi \quad (3.18)$$

where  $\phi$  is the determinant of a  $2n \times 2n$  matrix (for  $n$  number of solitons) given by

$$\phi = \det \left[ \left( x + p_k y + p_k^2 t + \theta_k \right) \delta_{kl} + (1 - \delta_{kl}) \frac{2\sqrt{3}i}{p_k - p_l} \right]. \quad (3.19)$$

Here  $\delta_{kl}$  is the Kronecker symbol, the indices take values  $k, l = 1, 2, \dots, 2n$ , while the complex constants  $p_k$  and  $\theta_k$  determine the velocity and the phase of each soliton, where  $p_{k+n} = \bar{p}_k$  and  $\theta_{k+n} = \bar{\theta}_k$ .

The one-soliton solution given by (3.18) and (3.19), when  $p_1 = i$  and  $\theta_1 = 60$ , has the simple expression

$$u(x, y, t) = 4 \frac{-(x - t + 60)^2 + y^2 + 3}{[(x - t + 60)^2 + y^2 + 3]^2}. \quad (3.20)$$

The corresponding configuration consists of a soliton which for  $t = 0$  is situated at the points  $(x, y) = (-60, 0)$  while for  $t \neq 0$  it travels along the  $x$ -axis without changing its shape and with constant velocities:  $(v_x, v_y) = (|p_1|^2, -2\Re(p_1))$ .

In addition, the corresponding multi-soliton solutions (3.18) and (3.19) are asymptotically free at  $t \rightarrow \pm\infty$  and move along their unperturbed trajectories without changing their shapes

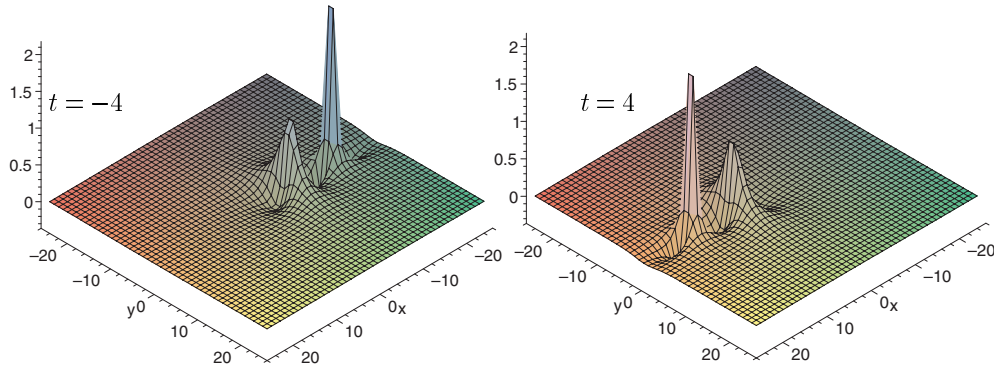


**Figure 2.** The two-soliton solution (3.18)–(3.19) of the KPI equation at different times with trivial scattering behaviour. The taller soliton passes through the smaller one with no phase shift or radiation.

and initial parameters after collision, i.e. they scatter trivially. Figure 2 represents snapshots of the two-soliton solution (3.18)–(3.19) for  $p_1 = i$ ,  $p_2 = 2i$  and  $\theta_1 = \theta_2 = 0$ .

Note that in the framework of plasma physics the classical KP equations suffer transverse instabilities according to the sign of the dispersive terms as well as possessing soliton solutions [16].

#### 4. Numerical simulations

In this section, we investigate numerically the existence of lattice multi-solitons using the fact that the lattice model asymptotically leads to an integrable equation. We use a numerical scheme by directly considering the lattice equations for the displacement  $u_{i,j}$  given by

$$\begin{aligned} \ddot{u}_{i,j} = & \alpha_1(u_{i+1,j} + u_{i-1,j} - 2u_{i,j}) + \alpha_2(2u_{i,j} - u_{i-1,j} - u_{i+1,j})(u_{i+1,j} - u_{i-1,j}) \\ & + \beta(u_{i,j+1} + u_{i,j-1} - 2u_{i,j}) - \delta(u_{i+2,j} - 4u_{i+1,j} + 6u_{i,j} - 4u_{i-1,j} + u_{i-2,j}) \\ & - \delta(u_{i,j+2} - 4u_{i,j+1} + 6u_{i,j} - 4u_{i,j-1} + u_{i,j-2}) - \eta(u_{i+4,j} - 4u_{i+2,j} + 6u_{i,j} \\ & - 4u_{i-2,j} + u_{i-4,j}) - \eta(u_{i,j+4} - 4u_{i,j+2} + 6u_{i,j} - 4u_{i,j-2} + u_{i,j-4}) \end{aligned} \quad (4.21)$$

which follow from (2.2) and (2.5). The numerical simulations are performed by employing a Runge–Kutta method of fourth order and imposing periodic boundary conditions, i.e.

$$u_{i+N,j} = u_{i,j} \quad u_{i,j+N} = u_{i,j} \quad (4.22)$$

where  $N$  is the number of particles along the boundaries of the square.

Note that it is not obvious if the solutions of the KPI equation will also be solutions of the lattice model. However, it was shown in [17] that this approach has been successfully considered in a one-dimensional lattice model. Specifically, when a one-dimensional lattice model with long-range interactions was considered (which, in the continuum, keeps its nonlocal behaviour) the long-time evolution of the localized waves is governed by an asymptotic integrable equation, the so-called Benjamin–Ono equation, which allows the explicit construction of moving kinks on the lattice. Accordingly, in this section we investigate the dynamical behaviour of the lattice model (4.21) numerically, using as initial conditions the one- and two-soliton solutions of the KPI integrable equation given in section 3.2.

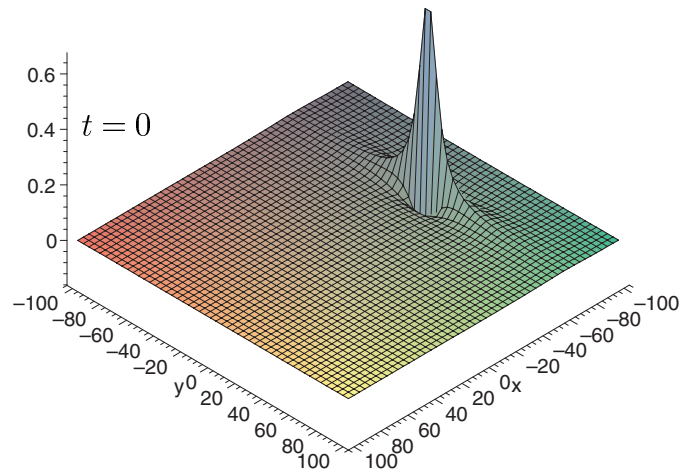


Figure 3. The one-soliton solution (4.25) for  $\varepsilon = 0.1$ .

By comparing the coefficients and the variables of equations (3.16) and (3.17), it is easy to see that (3.16) transforms to (3.17) when

$$\begin{aligned} \bar{\alpha} &= 3 & x &\rightarrow \xi = x - ct \\ \beta &= 1 & y &\rightarrow Y = \varepsilon^{1/2}y \\ \bar{\delta}_L &= 1 & t &\rightarrow T = -\varepsilon t/2c. \end{aligned} \quad (4.23)$$

Then it is a matter of simple algebra to observe that, due to (4.23), the parameters of the discrete model given by (3.12) and (3.13) are equal to

$$\alpha_2 = 3\varepsilon \quad \delta = \frac{c^2}{12} - 16\eta - \varepsilon \quad (4.24)$$

and, thus, the only arbitrary parameters of the lattice model are the following three:  $\varepsilon$ ,  $c$  and  $\eta$ . Due to numerical simplicity, in all our simulations we have chosen the following fixed values for: (i) the small parameter related to the weak nonlinearity  $\varepsilon = 0.1$ , (ii) the lattice spacing  $h = 1$ , (iii) the total number of the lattice points  $N = 100$ , (iv) the time step  $dt = 0.1$  and (v) the total number of time steps is equal to 5000 points. However, different values for the above parameters give qualitatively the same results as long as  $\varepsilon < 1$ .

#### 4.1. Dynamics of one soliton

Firstly, we investigate the time evolution of a single solution where the configuration given by (3.20) has been considered under the change of variables (4.23). More precisely, the initial conditions for the displacements and the velocities of each lattice particle, in the case of the one soliton (3.20), are given by the analytic expression

$$u(x, y, t)|_{t=0} = 4 \frac{-(x - ct + \varepsilon t/2c + 60)^2 + \varepsilon y^2 + 3}{[(x - ct + \varepsilon t/2c + 60)^2 + \varepsilon y^2 + 3]^2} \Big|_{t=0} \quad (4.25)$$

and its time derivative, respectively. Figure 3 illustrates snapshot of the displacement  $u_{i,j}(t)$  at  $t = 0$ .

We have run our simulations for different values of the parameters ( $c$ ,  $\eta$ ) and investigate whether the initial lattice soliton relaxes and propagates in the lattice space with small (or no)



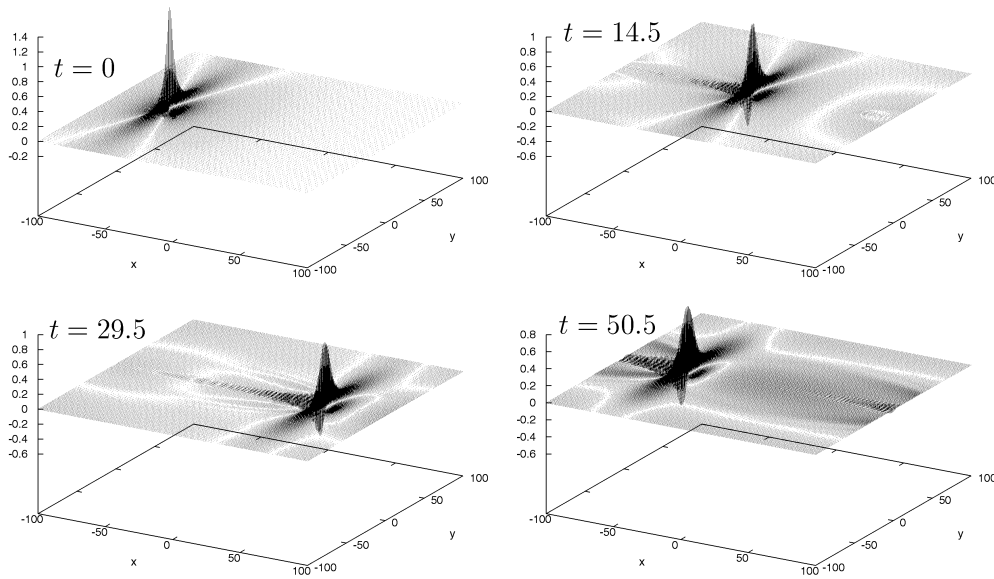


**Figure 4.** The time evolution of the lattice one soliton for  $c = 4$  and  $\eta = -1/60$ .

oscillations. This phenomenon occurs only for a specific range of values of the aforementioned parameters which give qualitatively the same results. In particular, due to [11], we know that the noncentral interaction parameter has to be negative and small. Our numerical study has shown that for values of the parameter  $\eta < 1/60$  and when the soliton velocity takes values in the range  $1 \leq c \leq 4$ , the loss of energy by radiation of small amplitude waves is small.

In figure 4, we display a full three-dimensional plot corresponding to the displacement  $u_{i,j}$  at four different times  $t = 0, 14.5, 29.5, 50.5$ . The initial conditions were created from one soliton placed at the position  $x_0 = -60$ . Figure 4 shows that the lattice soliton is stable throughout the numerical simulations; more precisely, its size is constant as it moves towards the plane without emitting any radiation. This process continues through several cycles, due to the periodic boundary conditions, without the occurrence of instabilities since the configuration settles to a single soliton which moves along the lattice grid.

Qualitatively, similar results have been found and studied in great detail in [17] for one-dimensional lattice kinks which are solutions of a nonlocal discrete model with long-range interactions. In that case, the lattice radiation was inversely proportional to the kink thickness.

#### 4.2. Two-soliton scattering

Next, we discuss the results of a numerical evolution of the full time-dependent lattice equations (4.21), in order to investigate the interaction and scattering of two solitons.

We take two solitons initially located at the origin (represented in figure 2) and evolve the equations of motion for different values of the soliton velocity  $c$  and the noncentral force parameter  $\eta$ . For values (approximately) in the following ranges:  $4 \leq c \leq 8$  and  $-1/30 \leq \eta \leq -1/360$ , the numerical simulations give qualitatively the same results, represented in figure 5.

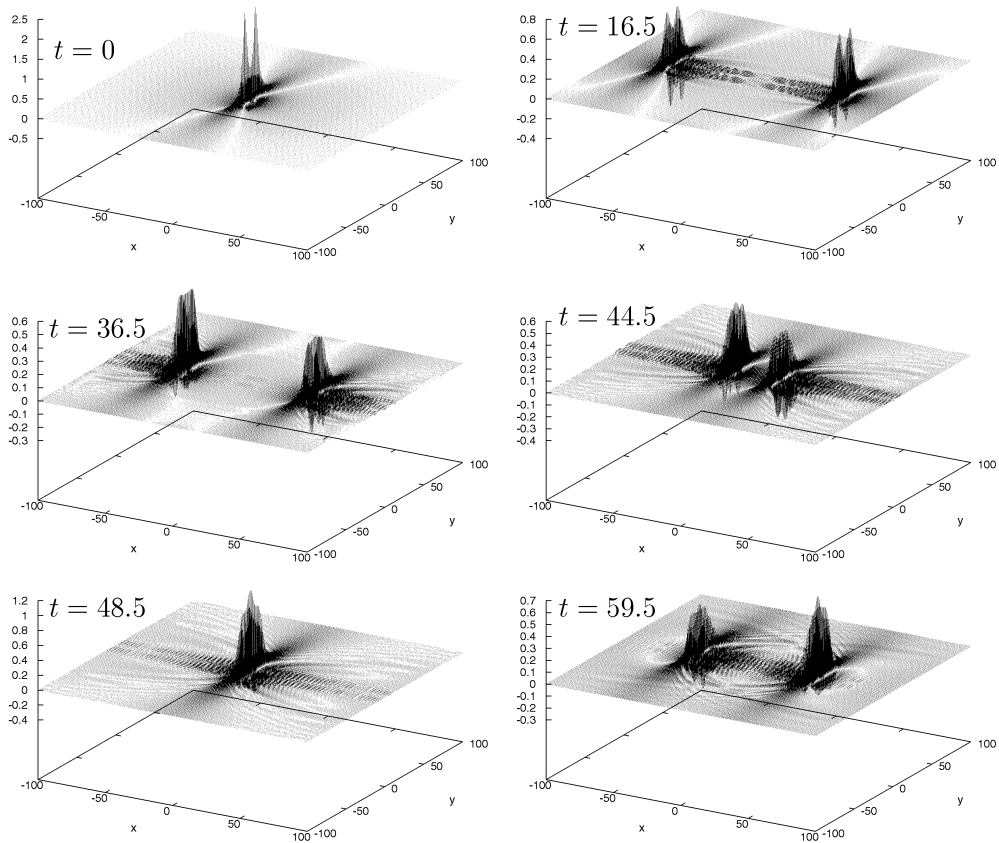


Figure 5. Two-soliton scattering for  $c = 4$  and  $\eta = -1/30$ .

From figure 5, we see that the two solitons which initially (at  $t = 0$ ) form a single large soliton travel with opposite velocities away from each other and then, due to the periodic boundary conditions, reappear at the edge of the lattice. Now, the two solitons head towards each other until they merge to form a single soliton again (at  $t = 48.5$ ) while after the collision, they continue their path with no phase shift or emission of radiation, i.e. they scatter trivially as the KPI solitons. In fact, a small amount of energy is radiated during the soliton motion as a result of the highly nonlinear deformation the solitons suffer in adjusting to the lattice grid. This radiation can be dealt with numerically by applying absorbing boundary conditions at the edge of the grid. The radiation emission is eliminated as the soliton velocity  $c$  increases. This scattering behaviour is continuous throughout a long time; specifically, we have run our simulations up to  $t_f = 500$  and although the lattice grid is covered from radiation the two solitons are easily distinguished.

To conclude, this approach can be extended to higher soliton numbers and we expect the results to be qualitatively like the ones obtained in the first two cases of the one- and two-soliton dynamics.

## 5. Conclusions

The main objective of the present work is to examine the long-time evolution of nonlinear localized waves of soliton type propagating on a two-dimensional lattice model. The starting

lattice model involves nonlinear (nonconvex lattice potential) and competing interactions which follow from noncentral interactions and play a key role in the existence and stability of the localized waves. Physically, the model describes the mechanism of micro-twinning of small ferroelastic domains in alloys suffering phase transformations, such as ferroelastic materials, martensitic transformations in shape memory alloys, etc.

The most interesting point of the study is that on the basis of a multi-scale technique, an asymptotic model for the long-time evolution of the nonlinear waves has been derived. This model is then governed by Kadomtsev–Petviashvili I equation which possesses soliton solutions. In order to check the analytical conjecture given by the asymptotic model, some numerical simulations have been performed (directly) on the discrete system. In fact, the numerical results describe the time evolution of one- and two-soliton solutions. It appears that the soliton solutions thus generated are particularly robust and stable which implies that the prediction provided by the asymptotic model is a good approximation of the solution of the discrete system. Therefore, we conclude with the observation that the KPI equation is an efficient asymptotic model to predict the existence of localized objects or nonlinear excitations of soliton type in a rather complex physical system.

Further extensions of the present work can be investigated. In particular, the dynamics of localized waves for a lattice model including higher-order nonlinear interatomic terms in the potential (fourth-order nonlinear term in discrete deformation, see equation (2.3)) can be considered; while it is worth investigating the influence of applied forces and damping on the nonlinear wave propagation and stability.

### Acknowledgments

This work has been performed in the framework of the TMR European Contract FMRXCT-960062: *Spatio-temporal instabilities in deformation and fracture mechanics, material science and nonlinear physics aspects*. TI acknowledges the Nuffield Foundation for a newly appointed lecturer award.

### References

- [1] Gaponov-Grekhov A V and Rabinovich M I 1990 *Phys. Today* **43** 30
- [2] Falo F, Bishop A R, Lomdahl P S and Horovitz B 1991 *Phys. Rev. B* **43** 8081
- [3] Parlinski K, Denoyer F and Eckold G 1991 *Phys. Rev. B* **43** 8411
- [4] Pouget J 1991 *Phase Transit.* **34** 105
- [5] Pouget J 1991 *Phys. Rev. B* **43** 3582
- [6] Pouget J 1992 *Phys. Rev. B* **46** 10554
- [7] Potapov A I, Pavlov I S, Gorshkov K A and Maugin G A 2001 *Wave Motion* **34** 83
- [8] Krumhansl J A and Gooding R J 1989 *Phys. Rev. B* **39** 3047
- [9] Krumhansl J A 1986 *Phys. Rev. Lett.* **56** 2696
- [10] Krumhansl J A 1992 *Solid State Commun.* **84** 251
- [11] Pouget J 1993 *Phys. Rev. B* **48** 864
- [12] Nayfeh A 1973 *Perturbation Methods* (New York: Wiley)
- [13] Kadomtsev B B and Petviashvili V I 1970 *Sov. Phys. Dokl.* **15** 539
- [14] Manakov S V, Zakharov V E, Bordag L A, Its A R and Matveev V B 1977 *Phys. Lett. A* **63** 205
- [15] Satsuma J and Ablowitz M J 1979 *J. Math. Phys.* **20** 1496
- [16] Laedke E W and Spatschek K H 1982 *J. Plasma Phys.* **28** 469
- [17] Ioannidou T, Pouget J and Aifantis E 2001 *J. Phys. A: Math. Gen.* **34** 4269